hepatocyte nuclear factor-4α in hepatoid foci: a case report with studies of previous cases. *Hum Pathol.* 2008;39:1115–1120.
18. Katzenstein ALA, Prioleau PG, Askin FB. The histologic spectrum and significance of clear-cell change in lung carcinoma. *Cancer.* 1980;45:943–947.
19. Takano T, Fukui T, Ohe Y, et al. EGFR mutations predict survival benefit from gefitinib in patients with advanced lung adenocarcinoma: a historical comparison of patients treated before and after gefitinib approval in Japan. *J Clin Oncol.* 2008;26:5589–5595.
20. Krypuy M, Newnham GM, Thomas DM, et al. High resolution melting analysis for the rapid and sensitive detection of mutations in clinical samples: KRAS codon 12 and 13 mutations in non-small cell lung cancer. *BMC Cancer.* 2006;6:295.
21. Sato S, Koike T, Yamato Y, et al. Resected well-differentiated fetal pulmonary adenocarcinoma and summary of 25 cases reported in Japan. *Jpn J Thorac Cardiovasc Surg.* 2006;54:539–542.
22. Howe M, Chapman A, Kerr K, et al. Neuroendocrine differentiation in non-small cell lung cancer and its relation to prognosis and therapy. *Histopathology.* 2005;46:195–201.
23. Ionescu DN, Treaba D, Gilks CB, et al. Nonsmall cell lung carcinoma with neuroendocrine differentiation - An entity of no clinical or prognostic significance. *Am J Surg Pathol.* 2007;31:26–32.
24. Segawa Y, Takata S, Fujii M, et al. Immunohistochemical detection of neuroendocrine differentiation in non-small-cell lung cancer and its clinical implications. *J Cancer Res Clin Oncol.* 2009;135:1055–1059.
25. Chang YC, Nagasue N, Abe S, et al. Comparison between the clinicopathologic features of AFP-positive and AFP-negative gastric cancers. *Am J Gastroenterol.* 1992;87:321–325.
26. Maitra A, Murakata LA, Albores-Saavedra J. Immunoreactivity for hepatocyte paraffin 1 antibody in hepatoid adenocarcinomas of the gastrointestinal tract. *Am J Clin Pathol.* 2001;115:689–694.
27. Kodama T, Kameya T, Hirota T, et al. Production of alpha-fetoprotein, normal serum proteins, and human chorionic gonadotropin in stomach cancer: Histologic and immunohistochemical analyses of 35 cases. *Cancer.* 1981;48:1647–1655.
28. Motoyama T, Aizawa K, Watanabe H, et al. alpha-Fetoprotein producing gastric carcinomas: a comparative study of three different subtypes. *Acta Pathol Jpn.* 1993;43:654–661.
29. Ushiku T, Uozaki H, Shinozaki A, et al. Glypican 3-expressing gastric carcinoma: distinct subgroup unifying hepatoid, clear-cell, and α-fetoprotein-producing gastric carcinomas. *Cancer Sci.* 2009;100:626–632.
30. Matsunou H, Konishi F, Jalal RE, et al. Alpha-fetoprotein-producing gastric carcinoma with enteroblastic differentiation. *Cancer.* 1994;73:534–540.
31. Ushiku T, Shinozaki A, Shibahara J, et al. SALL4 represents fetal gut differentiation of gastric cancer, and is diagnostically useful in distinguishing hepatoid gastric carcinoma from hepatocellular carcinoma. *Am J Surg Pathol.* 2010;34:533–540.
32. Hishinuma M, Ohashi K, Yamauchi N, et al. Hepatocellular oncofetal protein, glypican 3 is a sensitive marker for α-fetoprotein-producing gastric carcinoma. *Histopathology.* 2006;49:479–486.
33. Kumashiro Y, Yao T, Aishima S, et al. Hepatoid adenocarcinoma of the stomach: histogenesis and progression in association with intestinal phenotype. *Hum Pathol.* 2007;38:857–863.
34. Mizoshita T, Tsukamoto T, Nakanishi H, et al. Expression of Cdx2 and the phenotype of advanced gastric cancers: relationship with prognosis. *J Cancer Res Clin Oncol.* 2003;129:727–734.
35. Kosaka T, Yatabe Y, Onozato R, et al. Prognostic implication of EGFR, KRAS, and TP53 gene mutations in a large cohort of Japanese patients with surgically treated lung adenocarcinoma. *J Thorac Oncol.* 2009;4:22–29.
36. Mitsudomi T, Kosaka T, Endoh H, et al. Mutations of the epidermal growth factor receptor gene predict prolonged survival after gefitinib treatment in patients with non-small-cell lung cancer with postoperative recurrence. *J Clin Oncol.* 2005;23:2513–2520.
37. Haneda H, Sasaki H, Lindeman N, et al. A correlation between EGFR gene mutation status and bronchioloalveolar carcinoma features in Japanese patients with adenocarcinoma. *Jpn J Clin Oncol.* 2006;36:69–75.
38. Brambilla E, Gazzeri S, Moro D, et al. Immunohistochemical study of p53 in human lung carcinomas. *Am J Pathol.* 1993;143:199–210.
39. Tsao MS, Aviel-Ronen S, Ding K, et al. Prognostic and predictive importance of p53 and RAS for adjuvant chemotherapy in non–small-cell lung cancer. *J Clin Oncol.* 2007;25:5240–5247.

© 2013 Lippincott Williams & Wilkins

Imai et al. World Journal of Surgical Oncology 2013, 11:113
http://www.wjso.com/content/11/1/113

WORLD JOURNAL OF SURGICAL ONCOLOGY

RESEARCH Open Access

Bronchioloalveolar invasion in non-small cell lung cancer is associated with expression of transforming growth factor-β1

Kazuhiro Imai[1*], Yoshihiro Minamiya[1], Akiteru Goto[2], Hiroshi Nanjo[2], Hajime Saito[1], Satoru Motoyama[1], Yusuke Sato[1], Satoshi Kudo[1], Shinogu Takashima[1], Yasushi Kawaharada[1], Nobuyasu Kurihara[1], Kimito Orino[1] and Jun-ichi Ogawa[1]

Abstract

Background: Adenocarcinoma in situ (AIS) and minimally invasive adenocarcinoma (MIA) with fibrous stromal invasion are newly introduced subtypes of small lung adenocarcinoma. AIS is a small localized adenocarcinoma in which growth is restricted to neoplastic cells along preexisting alveolar structures without fibrous stromal invasion. In MIA, by contrast, tumor cells have infiltrated the myofibroblastic stroma. Transforming growth factor (TGF)-β is known to be produced by progressor tumors, and excessive TGF-β contributes to a pathological excess of tissue fibrosis. TGF-β1 is the most abundant isoform, and its expression is a key event fostering tumor invasion and metastasis. We therefore analyzed the relationship between TGF-β1 expression and clinicopathological microinvasion in patients with small lung adenocarcinoma.

Methods: The study participants were 45 patients who underwent curative surgery for AIS and MIA 3 cm or less in size. Those tumors were assessed based on immunohistochemical staining using anti-TGF-β1 antibody. The TGF-β1 status was assessed immunohistochemically using the Allred 8-unit system.

Results: The rates of TGF-β1 positivity in the AIS and MIA groups were 27.3% and 65.2%, respectively ($P < 0.05$). The median of Allred score was 0.5 (range 0–5) in the AIS group and 3.0 (range 0–6) in the MIA group ($P = 0.0017$).

Conclusions: We suggest that TGF-β1 expression is likely to be significantly stronger in patients with MIA than in those with AIS, and the increased expression may be associated with minimal invasion and infiltration of the myofibroblastic stroma.

Keywords: Adenocarcinoma in situ, Lung cancer, Minimally invasive adenocarcinoma, Transforming growth factor-β1

Background

Adenocarcinoma is the most common histological type among lung cancers. As with malignancies in other organs such as the breast and cervix, where carcinomas are defined as non-invasive, micro-invasive or invasive, the extent of the invasive component in lung adenocarcinomas is associated with clinical outcomes [1]. To address advances in oncology, molecular biology, pathology, radiology, and surgery, an international multidisciplinary classification was sponsored by the International Association for the Study of Lung Cancer (IASLC), the American Thoracic Society, and the European Respiratory Society [2]. Adenocarcinoma in situ (AIS) and minimally invasive adenocarcinoma (MIA) with fibrous stromal invasion are newly introduced subtypes, while the older term of bronchioloalveolar carcinoma does no longer exist according to new IASLC classification of lung adenocarcinoma. AIS is a localized small (≤3 cm) adenocarcinoma, the growth of which is restricted to neoplastic cells along preexisting alveolar structures without stromal, vascular or pleural invasion. Papillary or micropapillary patterns and intra-alveolar tumor cells are absent. MIA is a small,

* Correspondence: i-karo@mui.biglobe.ne.jp
[1]Department of Chest, Breast and Endocrine Surgery, Akita University Graduate School of Medicine, 1-1-1 Hondo, Akita City 010-8543, Japan
Full list of author information is available at the end of the article

BioMed Central

© 2013 Imai et al.; licensee BioMed Central Ltd. This is an Open Access article distributed under the terms of the Creative Commons Attribution License (http://creativecommons.org/licenses/by/2.0), which permits unrestricted use, distribution, and reproduction in any medium, provided the original work is properly cited.

solitary adenocarcinoma growing in a predominantly lepidic pattern and showing ≤5 mm invasion in its greatest dimension at any one focus. If these tumors are completely resected, there will be 100% or near 100% disease-specific survival.

Transforming growth factor (TGF)-β reportedly promotes cancer metastasis by affecting the tumor microenvironment in a manner that facilitates tumor cell invasion [3,4]. Several tumors, including those arising in the lung [5-7], express high levels of TGF-β, which correlate with tumor progression and clinical prognosis. Humans express three highly homologous isoforms of TGF-β (TGF-βs 1, 2, and 3), which share 70% sequence identity in their biologically active C-terminal regions, and all of which bind to the same receptor complex and activate the same downstream signaling pathways. TGF-β1 is the most abundant and most extensively studied isoform [8].

We previously showed that tumor-derived TGF-β1 causes a reduction in the number of dendritic cells within the sentinel lymph node in lung cancer [9]. Our findings also suggest that TGF-β1 29T>C genetic polymorphism is associated with lymph node metastasis in patients with adenocarcinoma of the lung [10]. In addition, we showed that overexpression of TGF-β1 by tumor cells promotes metastasis into tumor-draining lymph nodes in mice, most likely by inhibiting dendritic cell migration from tumors towards tumor-draining nodes [11]. Collectively, these results suggest that TGF-β1 is a key mediator fostering tumor invasion and metastasis. We therefore analyzed the relationship between TGF-β1 expression and clinicopathological microinvasion in patients with small lung adenocarcinoma.

Methods

Patients

In total, 453 patients who had undergone major pulmonary resections for non-small cell lung cancer (NSCLC) were enrolled in the study. Among them, 45 patients (10.1%) with NSCLC had AIS and MIA subtypes of small lung adenocarcinoma 3 cm or less in size. All had undergone surgery in the Department of Chest, Breast and Endocrine Surgery, University Hospital of Akita University Graduate School of Medicine, between January 2004 and December 2011. This study was approved by our institutional review boards, and written informed consent was obtained from all patients. The patients' characteristics are listed in Table 1. The 7th edition of the TNM staging system was used for evaluation [12].

Pathology

Surgically resected specimens were fixed in 10% formalin and routinely processed for paraffin embedding. Histological sections were cut into 4-mm slices, which were then stained with hematoxylin and eosin (HE) and elastica Masson using standard methods, and were reviewed by two pathologists (A.G. and H.N.). Experienced pathologists diagnosed the subtypes of the primary tumors according to IASLC/American Thoracic Society/European Respiratory Society International Multidisciplinary Classification of adenocarcinoma [2]. Diagnosis of AIS or MIA was based on the HE staining (Figure 1).

Table 1 Clinical details of all patients who underwent pulmonary resection for small lung adenocarcinoma

	AIS	MIA	*P* value
n	22	23	
Age (year)	63±11.9	67±9.3	0.232
Gender (M/F)	8/14	8/15	0.675
Tumor size	11.1±3.7	15.0±5.6	0.022*
Nodal involvement			0.162
N0	22	22	
N1	0	1	
N2	0	0	
Stage			0.243
IA	22	22	
IB	0	0	
IIA	0	1	

AIS Adenocarcinoma in situ, *MIA* Minimally invasive adenocarcinoma, *P <0.05.

Immunohistochemistry of TGF-β1 in small lung adenocarcinoma

After reviewing HE-stained sections of the tumor specimens, we selected blocks from the central regions of the tumors for further study. The paraffin-embedded tumor tissues were cut into 4-μm-thick sections and deparaffinized. Small lung adenocarcinomas were then assessed based on standard immunohistochemical (IHC) staining using goat polyclonal anti-TGF-β1 (1:50 dilution; Santa Cruz Biotechnology, Inc., Santa Cruz, CA, USA), anti-goat horseradish peroxidase (1:100 dilution), and diaminobenzidene stain (Figure 2). The TGF-β1 staining was scored using the Allred 8-unit system with the combination of a proportion score from 0 to 5 and an intensity score from 0 to 3. The proportion score included the fraction of positively stained tumor cells and was as follows: 0 = none, 1 ≤1/100; 2 = 1/100 to 1/10; 3 = 1/10 to 1/3; 4 = 1/3 to 2/3; 5 ≥2/3. The staining intensity score was as follows: 0 = none; 1 = weak; 2 = intermediate; 3 = strong [13,14].

Immunohistochemical detection of micrometastasis and isolated tumor cells in dissected lymph nodes

Isolated tumor cells and lymph node micrometastasis were assessed in all patients based on HE staining and IHC using AE1/AE3 antibodies. One section of the maximum cut surface of each lymph node was immunohistochemically

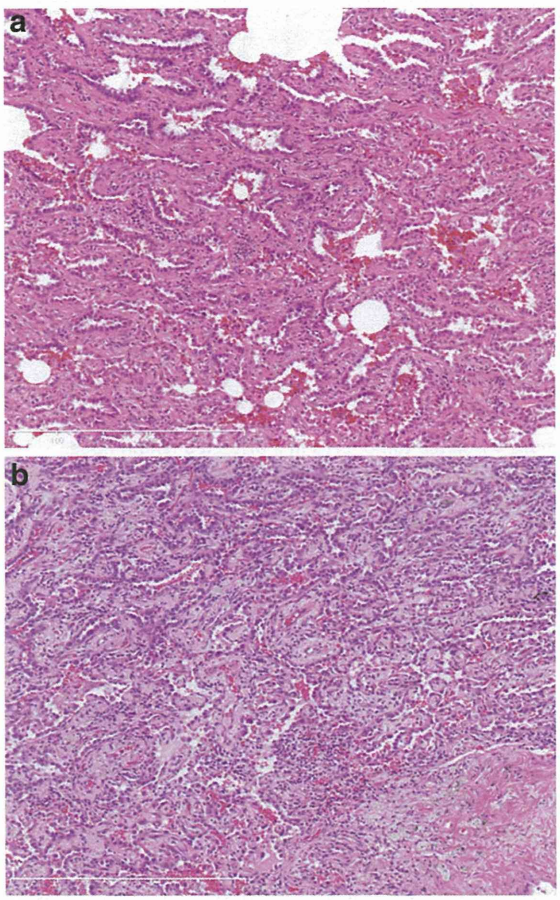

Figure 1 International multidisciplinary classification of lung adenocarcinoma. (**a**) Adenocarcinoma in situ. Histologic specimen showing a tumor with atypical pneumocytes proliferating along slightly thickened but preserved alveolar walls; (**b**) Minimally invasive adenocarcinoma. Histologic specimen of a tumor exhibiting a bronchioloalveolar growth pattern with minimal invasion. The tumor is invading in the fibrous stroma.

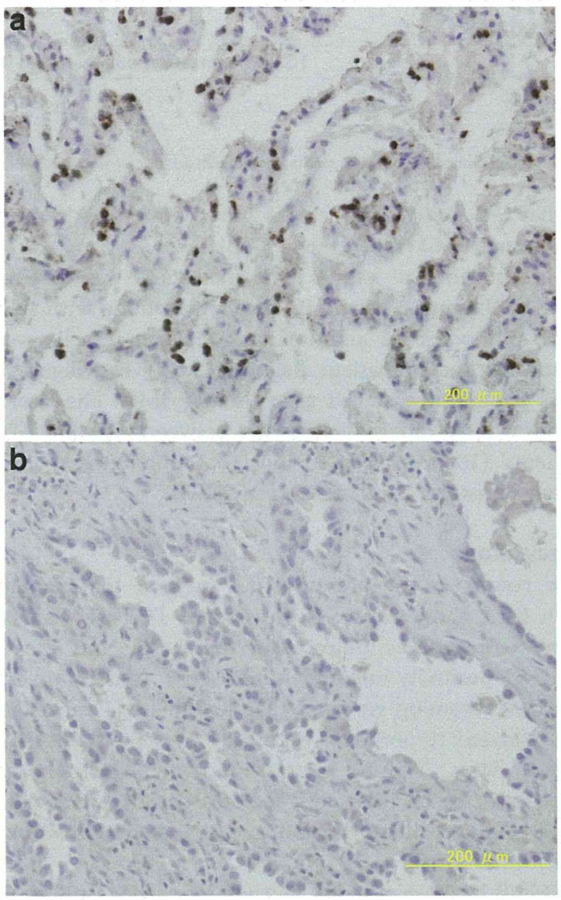

Figure 2 Immunostaining adenocarcinoma in situ and minimally invasive adenocarcinoma using an anti-TGF-β1 antibody. (**a**) TGF-β1-positive MIA sample. TGF-β1-positive cells are stained brown. TGF-β1-positive cells are predominantly observed in the tumor itself. This sample has an Allred score of 6/8; (**b**) TGF-β1 -negative AIS sample. This sample has an Allred score of 0/8. TGF: Transforming growth factor; AIS: Adenocarcinoma in situ; MIA: Minimally invasive adenocarcinoma.

labeled with AE1/AE3 monoclonal mouse anti-human cytokeratin clones using an EnVision system (DAKO Corporation, Carpinteria, CA, USA), which was used to detect the presence of micrometastases and isolated tumor cells. A result was considered positive if positive cell clusters or individual cells with the appropriate tumor cell morphology were recognized. As proposed by the 7th edition of the TNM staging system [12], isolated tumor cells were not considered as positive, but were defined as pN0(i+) in this study.

Statistics

Group data were expressed as means ± SD. Categorical data were compared using the χ^2 test. The significance of individual differences was evaluated using the Wilcoxon test. Values of P <0.05 were considered to be significant. JMP IN 8.0.2 software (SAS Institute, Cary, NC, USA) was used for all statistical evaluations.

Results

There were no differences between the AIS and MIA groups with respect to age, gender, nodal involvement or pathological stage; however, tumor size was greater in the MIA group than the AIS group (Table 1). Table 2 shows the incidence of TGF-β1 expression detected upon immunohistochemical examination in the AIS and MIA groups. Figure 3 shows the differences in TGF-β1 immunostaining between AIS and MIA scored using the Allred method. The rate of TGF-β1 positivity was significantly (P <0.05) higher in the MIA group (65.2%; 15/23) than the AIS group (27.3%; 6/22). Similarly, the median Allred score for TGF-β1 expression was significantly

Table 2 Incidence of TGF-β1 expression in the AIS and MIA groups

	TGF-β1 expression positive stain (%)
AIS (n=22)	27.3
MIA (n=23)	65.2*

AIS Adenocarcinoma in situ, *MIA* Minimally invasive adenocarcinoma, *P <0.05.

higher (P = 0.0017) in the MIA group than the AIS group (3.0 (range 0–6) *vs.* 0.5 (range 0–5)).

One instance of lymph node metastasis was detected in the MIA group using HE and IHC staining with AE1/AE3 antibodies. In addition, isolated tumor cells were found in a second patient diagnosed with MIA (Figure 4). This patient was staged as pT1aN0(i+)M0. The overall survival rates differed somewhat between AIS and MIA patients (100% *vs.* 89.5%), but that difference did not reach statistical significance (P = 0.093).

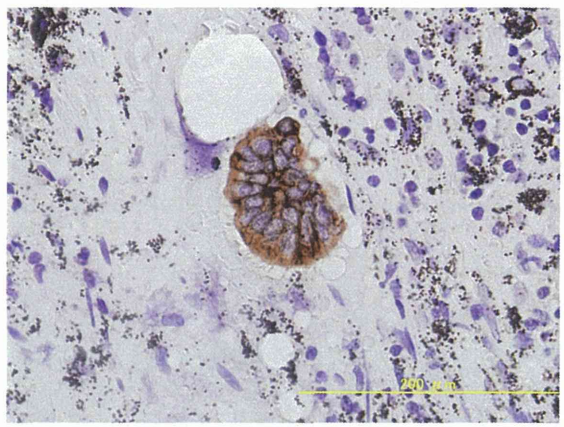

Figure 4 Isolated tumor cells in a dissected lymph node. Isolated tumor cells were detected by immunostaining using anti-cytokeratin antibody in a patient diagnosed with MIA. The patient's pathological stage was pT1aN(i+)M0, Stage IA.

Discussion

The results of the present study suggest that patients with MIA show greater expression of TGF-β1 than patients with AIS, as indicated by the significantly greater TGF-β1 positivity rate and Allred score. In addition, HE and IHC staining revealed that lymph node metastasis and isolated tumor cells were only present in the MIA group. Thus, TGF-β1 expression by adenocarcinomas appears to be an important factor associated with clinicopathological microinvasion in patients with small lung adenocarcinoma.

TGF-β increases the invasiveness of cancer cells by increasing their proteolytic activity and promoting their binding to cell-adhesion molecules [15]. In an earlier study, we demonstrated that tumor-derived TGF-β1 induces dendritic cell apoptosis within lymph nodes in non-small cell lung cancer [9], and that overexpression of TGF-β1 by tumor cells promotes lymph node metastasis in mice [11]. Consistent with those findings, the effects of TGF-β1 on angiogenesis, stroma formation and immune function appear to further support tumor progression and invasion [16,17]. AIS is a small localized adenocarcinoma in which growth is restricted to neoplastic cells along preexisting alveolar structures without fibrous stromal invasion. In MIA, by contrast, tumor cells have infiltrated the myofibroblastic stroma. In many diseases, excessive TGF-β contributes to a pathological excess of tissue fibrosis that compromises normal organ function, a topic that has been the subject of several reviews [18-20]. However, we provide no direct evidence of the mechanism by which TGF-β1 increases tissue fibrosis in MIAs.

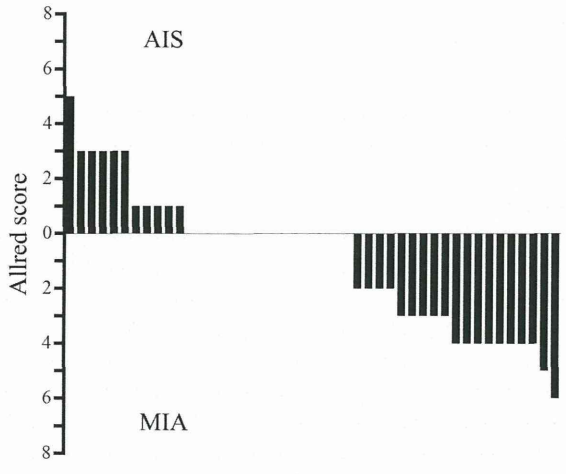

Figure 3 Allred score system devised to score results from immunohistochemical tests of TGF-β1. Differences in TGF-β1 immunostaining between AIS and MIA scored using the Allred method; *P <0.05.

The Noguchi classification [21] is predictive of outcome in patients with small adenocarcinomas, with type D, E, and F tumors showing a worse outcome than the other tumor types. However, the majority of small adenocarcinomas are classified as type C, so that subclassification of type C tumors does seem necessary. Tumors that meet the criteria for AIS were formerly classified as bronchioloalveolar carcinoma based on the strict definition of type A and type B adenocarcinomas from the 1995 Noguchi classification [21]. MIAs are tumors showing lepidic growth and a small (≤5 mm) area of invasion. The MIA invades areas of stromal fibrosis in an acinar pattern. Nearly all type C adenocarcinomas can be classified as MIAs. The outcome of patients with adenocarcinomas with diameters of 2 cm or less can be predicted using the following scoring system based on three histological criteria: 1) the tumor is lymphovascular

invasion-positive; 2) the non-bronchioloalveolar carcinoma component is >10 mm in diameter; and 3) the percentage of the solid, cribriform, and/or papillary components is ≥30% of the entire tumor volume [22]. Patients whose MIAs have a non-bronchioloalveolar carcinoma component ≤5 mm show 100% survival [22,23]. Consistent with that finding, no difference in survival was observed between AIS and MIA in the present study. However, nodal involvement was observed in 2 of 23 patients with MIA. We therefore suggest that it would be problematic to conduct limited surgery for MIA patients with micrometastasis or isolated tumor cells, though some MIAs may be candidates for limited surgery.

Conclusions

In conclusion, our findings suggest that patients with MIAs have both a significantly greater rate of TGF-β1 positivity and higher TGF-β1 Allred scores than patients with AIS. However, because we do not provide direct evidence of the mechanism by which TGF-β1 increases tissue fibrosis in MIAs, and we examined only a limited number of patients, further studies will be needed to more precisely define the role played by tumor-derived TGF-β1 in determining the invasiveness of adenocarcinoma of the lung.

Abbreviations

AIS: Adenocarcinoma in situ; HE: hematoxylin and eosin; IHC: immunohistochemical; MIA: Minimally invasive adenocarcinoma; NSCLC: Non-small cell lung cancer; TGF: Transforming growth factor.

Competing interests

The authors declare that they have no competing interests.

Authors' contributions

KI performed immunohistochemical staining, analyzed data and wrote the paper. YM designed the research. AG and HN evaluated histological staining and diagnosed lymph node metastasis. HS, SM, YS, SK, ST, YK, and NK performed and contributed to data analysis. KO contributed to histological diagnosis. JO contributed to clinical design and data analysis. All authors read and approved the final manuscript.

Author details

[1]Department of Chest, Breast and Endocrine Surgery, Akita University Graduate School of Medicine, 1-1-1 Hondo, Akita City 010-8543, Japan. [2]Department of Pathology, Akita University Graduate School of Medicine, 1-1-1 Hondo, Akita City 010-8543, Japan.

Received: 22 November 2012 Accepted: 13 May 2013
Published: 25 May 2013

References

1. Toonkel RL, Borczuk AC, Powell CA: **TGF-beta signaling pathway in lung adenocarcinoma invasion.** *J Thorac Oncol* 2010, **5**:153–157.
2. Travis WD, Brambilla E, Noguchi M, Nicholson AG, Geisinger KR, Yatabe Y, Beer DG, Powell CA, Riely GJ, Van Schil PE, Garg K, Austin JH, Asamura H, Rusch VW, Hirsch FR, Scagliotti G, Mitsudomi T, Huber RM, Ishikawa Y, Jett J, Sanchez-Cespedes M, Sculier JP, Takahashi T, Tsuboi M, Vansteenkiste J, Wistuba I, Yang PC, Aberle D, Brambilla C, Flieder D, *et al*: **International association for the study of lung cancer/american thoracic society/ european respiratory society international multidisciplinary classification of lung adenocarcinoma.** *J Thorac Oncol* 2011, **6**:244–285.
3. Giampieri S, Pinner S, Sahai E: **Intravital imaging illuminates transforming growth factor beta signaling switches during metastasis.** *Cancer Res* 2010, **70**:3435–3439.
4. Korpal M, Kang Y: **Targeting the transforming growth factor-beta signaling pathway in metastatic cancer.** *Eur J Cancer* 2010, **46**:1232–1240.
5. Barthelemy-Brichant N, David JL, Bosquée L, Bury T, Seidel L, Albert A, Bartsch P, Baugnet-Mahieu L, Deneufbourg JM: **Increased TGF beta1 plasma level in patients with lung cancer: potential mechanisms.** *Eur J Clin Invest* 2002, **32**:193–198.
6. Lee JC, Lee KM, Kim DW, Heo DS: **Elevated TGF-beta1 secretion and down-modulation of NKG2D underlies impaired NK cytotoxicity in cancer patients.** *J Immunol* 2004, **172**:7335–7340.
7. Domagala-Kulawik J, Hoser G, Safianowska A, Grubek-Jaworska H, Chazan R: **Elevated TGF-beta1 concentration in bronchoalveolar lavage fluid from patients with primary lung cancer.** *Arch Immunol Ther Exp (Warsz)* 2006, **54**:143–147.
8. Flanders KC, Wakefield LM: **Transforming growth factor-(beta)s and mammary gland involution; functional roles and implications for cancer progression.** *J Mammary Gland Biol Neoplasia* 2009, **14**:131–144.
9. Ito M, Minamiya Y, Kawai H, Saito S, Saito H, Nakagawa T, Imai K, Hirokawa M, Ogawa J: **Tumor-derived TGF beta-1 induces dendritic cell apoptosis in the sentinel lymph node.** *J Immunol* 2006, **176**:5637–5643.
10. Minamiya Y, Miura M, Hinai Y, Saito H, Ito M, Ono T, Toda H, Motoyama S, Ogawa J: **Transforming growth factor-β1 29T>C genetic polymorphism is associated with lymph node metastasis in patients with adenocarcinoma of the lung.** *Tumour Biol* 2010, **31**:437–441.
11. Imai K, Minamiya Y, Koyota S, Ito M, Saito H, Sato Y, Motoyama S, Sugiyama T, Ogawa J: **Inhibition of dendritic cell migration by transforming growth factor-β1 increases tumor-draining lymph node metastasis.** *J Exp Clin Cancer Res* 2012, **31**:3.
12. Sobin LH, Gospodarowicz MK, Wittekind C: *(Eds): TNM Classification of Malignant Tumours.* 7th edition. New York: Wiley-Blackwell; 2009.
13. Allred DC, Harvey JM, Berardo M, Clark GM: **Prognostic and predictive factors in breast cancer by immunohistochemical analysis.** *Mod Pathol* 1998, **11**:155–168.
14. Coppola D, Szabo M, Boulware D, Muraca P, Alsarraj M, Chambers AF, Yeatman TJ: **Correlation of osteopontin protein expression and pathological stage across a wide variety of tumor histologies.** *Clin Cancer Res* 2004, **10**:184–190.
15. Maehara Y, Kakeji Y, Kabashima A, Emi Y, Watanabe A, Akazawa K, Baba H, Kohnoe S, Sugimachi K: **Role of transforming growth factor-b 1 in invasion and metastasis in gastric carcinoma.** *J Clin Oncol* 1999, **17**:607–614.
16. Hasegawa Y, Takanashi S, Kanehira Y, Tsushima T, Imai T, Okumura K: **Transforming growth factor-beta1 level correlates with angiogenesis, tumor progression, and prognosis in patients with nonsmall cell lung carcinoma.** *Cancer* 2001, **91**:964–971.
17. Weeks BH, He W, Olson KL, Wang XJ: **Inducible expression of transforming growth factor beta1 in papillomas causes rapid metastasis.** *Cancer Res* 2001, **61**:7435–7443.
18. Bonewald LF: **Regulation and regulatory activities of transforming growth factor beta.** *Crit Rev Eukaryot Gene Expr* 1999, **9**:33–44.
19. Border WA, Noble NA: **Transforming growth factor beta in tissue fibrosis.** *N Engl J Med* 1994, **331**:1286–1292.
20. Moses HL, Yang EY, Pietenpol JA: **TGF-beta stimulation and inhibition of cell proliferation: new mechanistic insights.** *Cell* 1990, **63**:245–247.
21. Noguchi M, Morikawa A, Kawasaki M, Matsuno Y, Yamada T, Hirohashi S, Kondo H, Shimosato Y: **Small adenocarcinoma of the lung. Histologic characteristics and prognosis.** *Cancer* 1995, **75**:2844–2852.
22. Maeshima AM, Tochigi N, Yoshida A, Asamura H, Tsuta K, Tsuda H: **Histological scoring for small lung adenocarcinomas 2 cm or less in diameter: a reliable prognostic indicator.** *J Thorac Oncol* 2010, **5**:333–339.
23. Sakurai H, Maeshima A, Watanabe S, Suzuki K, Tsuchiya R, Maeshima AM, Matsuno Y, Asamura H: **Grade of stromal invasion in small adenocarcinoma of the lung: histopathological minimal invasion and prognosis.** *Am J Surg Pathol* 2004, **28**:198–206.

doi:10.1186/1477-7819-11-113
Cite this article as: Imai *et al.*: Bronchioloalveolar invasion in non-small cell lung cancer is associated with expression of transforming growth factor-β1. *World Journal of Surgical Oncology* 2013 **11**:113.

Identification of CCDC6-RET Fusion in the Human Lung Adenocarcinoma Cell Line, LC-2/ad

Daisuke Matsubara MD, PhD,† Yoshihiko Kanai,‡ Shumpei Ishikawa, MD, PhD,§ Shiori Ohara, BSc,* Taichiro Yoshimoto, MD, PhD,* Takashi Sakatani, MD, PhD,* Sachiko Oguni,* Tomoko Tamura,* Hiroaki Kataoka, MD, PhD,‖ Shunsuke Endo, MD, PhD,‡ Yoshinori Murakami, MD, PhD,† Hiroyuki Aburatani, MD, PhD,¶ Masashi Fukayama, MD, PhD,§ and Toshiro Niki, MD, PhD**

Rearranged during transfection (*RET*) fusions have been newly identified in approximately 1% of patients with primary lung tumors. However, patient-derived lung cancer cell lines harboring *RET* fusions have not yet been established or identified, and therefore, the effectiveness of an RET inhibitor on lung tumors with endogenous *RET* fusion has not yet been studied. In this study, we report identification of *CCDC6-RET* fusion in the human lung adenocarcinoma cell line LC-2/ad. LC-2/ad showed distinctive sensitivity to the RET inhibitor, vandetanib, among 39 non–small lung cancer cell lines. The xenograft tumor of LC-2/ad showed cribriform acinar structures, a morphologic feature of primary *RET* fusion–positive lung adenocarcinomas. LC-2/ad cells could provide useful resources to analyze molecular functions of RET-fusion protein and its response to *RET* inhibitors.

Key Words: RET fusion, Lung adenocarcinoma, Cell line, Vandetanib.

(*J Thorac Oncol.* 2012;7: 1872–1876)

Lung cancer is the leading cause of cancer mortality in developed countries. Molecularly targeted therapy is a new therapeutic modality now under intense investigation.[1] *KRAS* mutations, epidermal growth factor receptor (*EGFR*) mutations, and anaplastic lymphoma receptor tyrosine kinase (*ALK*) fusions are well-known driver mutations identified in individuals with lung adenocarcinoma. Molecular analyses have demonstrated that *EGFR*-mutated non–small-cell lung tumors are usually sensitive to the EGFR inhibitors gefitinib and erlotinib, and *ALK* fusion non–small-cell lung tumors are sensitive to the ALK inhibitor crizotinib. Lung tumors with *ROS1* fusions also respond to crizotinib.[2]

Recently, several independent studies newly identified *RET* fusions (*KIF5B-RET* or *CCDC6-RET*) in approximately 1% of patients with primary lung tumors.[3–9] *RET* fusions were mutually exclusive of *EGFR*, *KRAS*, and *ALK* mutations. Although these studies suggested that RET kinase inhibitors would be effective for a subgroup of lung tumors harboring *RET* fusions, the clinical benefits of RET kinase inhibitors in these patients have not been clarified yet. Studies using patient-derived lung cancer cell lines harboring *RET* fusions are now needed to decide the best optimal drug treatments; however, lung cancer cell lines with endogenous *RET* fusions have not been established nor identified to date.[10]

In this study, we found that a lung adenocarcinoma cell line, LC-2/ad, harbored *CCDC6-RET* fusion, and examined its sensitivity to vandetanib, a multikinase inhibitor of RET, vascular endothelial growth factor receptor-2, and EGFR. To the best of our knowledge, this is the first report to identify a patient-derived lung cancer cell line harboring *RET* fusion and demonstrate its sensitivity to a RET kinase inhibitor. The availability of this cell line would facilitate studies on optimal drug treatments and the biological properties of *RET* fusion–positive lung adenocarcinomas.

MATERIALS AND METHODS

Cell Lines and Medium

We used 39 non–small-cell lung cancer cell lines, 34 adenocarcinoma cell lines (H23, H292, H358, H441, H522, H596, H650, H1395, H1648, H1650, H1651, H1703, H1781, H1793, H1838, H1975, H1993, H2009, H2087, H2228, H2405, HCC827, HCC4006, Calu-3, A549, ABC1, PC3, VMRC-LCD, RELF-LC-Ad1, RELF-LC-Ad2, HLC-1, LC-2/ad, RERF-LC-KJ, and L27), four large-cell carcinoma cell lines (Lu65, H460, H661, and H1299), and one adenosquamous cell line (H596). Detailed information on

*Department of Pathology, Division of Integrative Pathology, Jichi Medical University, Shimotsuke, Tochigi, Japan; †Department of Cancer Biology, Division of Molecular Pathology, The Institute of Medical Science, The University of Tokyo, Minato-ku, Tokyo; ‡Department of Surgery, Division of General Thoracic Surgery, Jichi Medical University, Tochigi, Japan; §Department of Human Pathology, Graduate School of Medicine, The University of Tokyo, Bunkyo-ku Tokyo; ‖Department of Pathology, Faculty of Medicine, University of Miyazaki, Miyazaki, Japan; and ¶Laboratory for Systems Biology and Medicine, Division of Genome Science, Research Center for Advanced Science and Technology, The University of Tokyo, Meguro-ku, Tokyo, Japan.

Disclosure: T.N. and D.M. are recipients of the AstraZeneca research award 2007. The authors declare no conflict of interest.

Address for correspondence: Toshiro Niki, MD, Department of Integrative Pathology, Jichi Medical University, 3311-1 Yakushiji, Shimotsuke-shi, Tochigi, 329–0498, Japan. E-mail: tniki@jichi.ac.jp00002012

Copyright © 2012 by the International Association for the Study of Lung Cancer

ISSN: 1556-0864/12/0712-1872

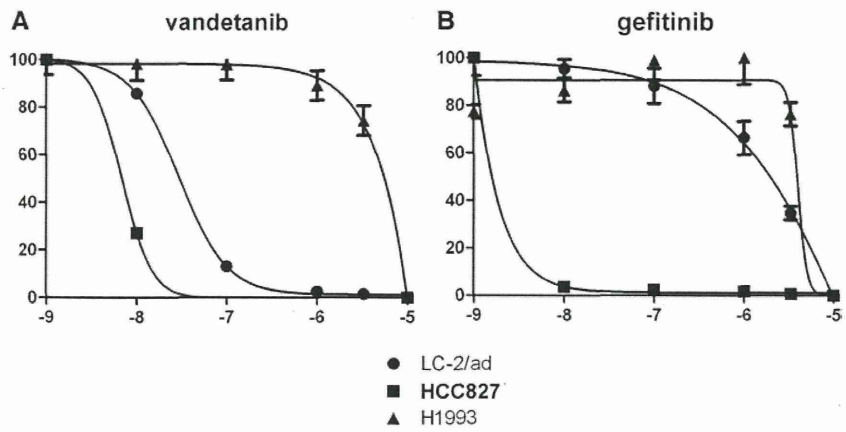

FIGURE 1. Dose-response curves of three cell lines, LC-2/ad, HCC827, and H1993. HCC827 harbors *EGFR* Exon 19 deletion (746–750) and H1993 expresses wild-type *EGFR*. The *x* axis indicates the log10 (concentration of vandetanib [*A*] and gefitinib [*B*]), and the *y* axis indicates the % of cell viability = (mean absorbance in test wells)/(mean absorbance in control well) × 100. *A*, LC-2/ad and HCC827 were sensitive to vandetanib (IC50 values were 2.9E-08 and 6.9E-09, respectively), but H1993 was resistant to vandetanib (IC50 value was 5.1E-04). *B*, HCC827 was sensitive to gefitinib (inhibitory concentration 50 value was 1.8E-10), but LC-2/ad and H1993 were resistant to gefitinib (inhibitory concentration 50 values were 1.8E-05 and 4.0E-06, respectively). EGFR, epidermal growth factor receptor.

the 39 cell lines is available in our previous reports.[11,12] Among the 39 cell lines, *EGFR* mutations were detected in five cell lines: HCC827, HCC4006, PC3, H1650, and H1975. *EGFR* mutation status of the five cell lines (Supplementary Table 1, Supplemental Digital Content 1, http://links.lww.com/JTO/A337). We have not checked the 39 cell lines for *ALK* fusion in our hands, but H2228 has been reported to harbor *ALK* fusion[13] (Supplementary Table 1, Supplemental Digital Content 1, http://links.lww.com/JTO/A337).

RET Fusion–Specific Polymerase Chain Reaction

We used fusion-specific reverse-transcriptase polymerase chain reaction (RT-PCR) with the forward primer, *CCDC6*-197F (5′-TGCAGCAAGAGAACAAGGTG-3′), the forward primer, *KIF5B*-867F (5′-ATCCAGTTCGTCCTGTTCAGAGC-3′), *KIF5B*-2265R (5′-AGCCACAGATCAGGAAAAGA-3′), and reverseprimer,*RET*-2381R(5′-CAGGCCCCATACAATTTGAT-3′), following the method by Takeuchi et al.[4]

Genetic and Protein Analysis of Cell Lines

The DNA, RNA, and cell lysates were prepared from cell lines by standard procedures. Experimental details of sequencing, copy number analyses, and Western blotting are given in our previous reports [11,12] (antibodies for Western blotting are listed in Supplementary Table 1, Supplemental Digital Content 1, http://links.lww.com/JTO/A337).

Cell-Proliferation Assay

Cell viability was measured by the Cell Counting Kit-8 assay (Dojindo, Kumamoto, Japan) following the manufacturer's instructions.[11]

Xenograft Tumor of LC-2/ad

We established a xenograft tumor of LC-2/ad by injecting cell suspensions (5×10^6) into the flank of a 6-week-old female severe combined immunodeficient mouse NOD C.B-17-Prkdc scid/J (NOD/SCID).

Immunohistochemistry

A formalin-fixed, paraffin-embedded xenograft tumor specimen of LC-2/ad was analyzed by immunohistochemistry using antibodies to RET, TTF-1, Napsin A, and thyroglobulin (sources of antibodies are given in Supplementary Table 2, Supplemental Digital Content 5, http://links.lww.com/JTO/A341).

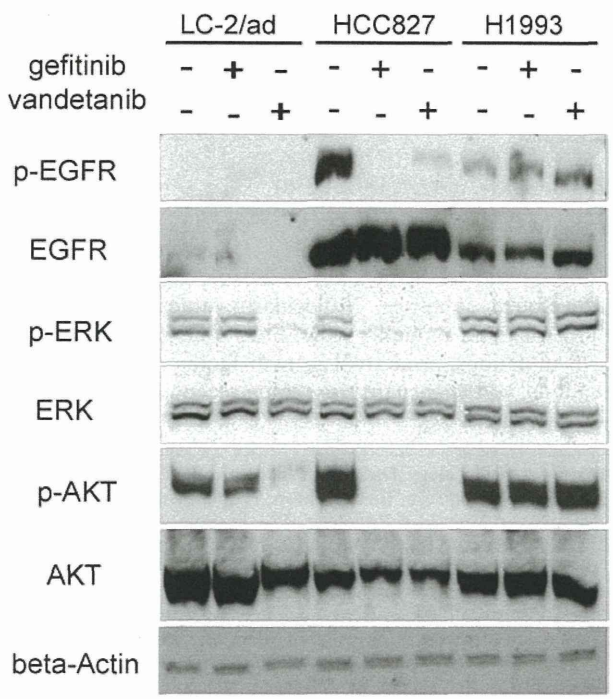

FIGURE 2. Effects of vandetanib and gefitinib on the phosphorylation levels of EGFR, ERK, and AKT in LC-2/ad, HCC827, and H1993. Gefitinib efficiently led to dephosphorylation of EGFR, ERK, and AKT in HCC827, but not in LC-2/ad and H1993. Vandetanib efficiently led to dephosphorylation of ERK and AKT in LC-2/ad and HCC827, but not in H1993.EGFR, EGFR, epidermal growth factor receptor; ERK, extracellular signal-regulated kinase; AKT, v-akt murine thymoma viral oncogene homolog 1.

Copyright © 2012 by the International Association for the Study of Lung Cancer

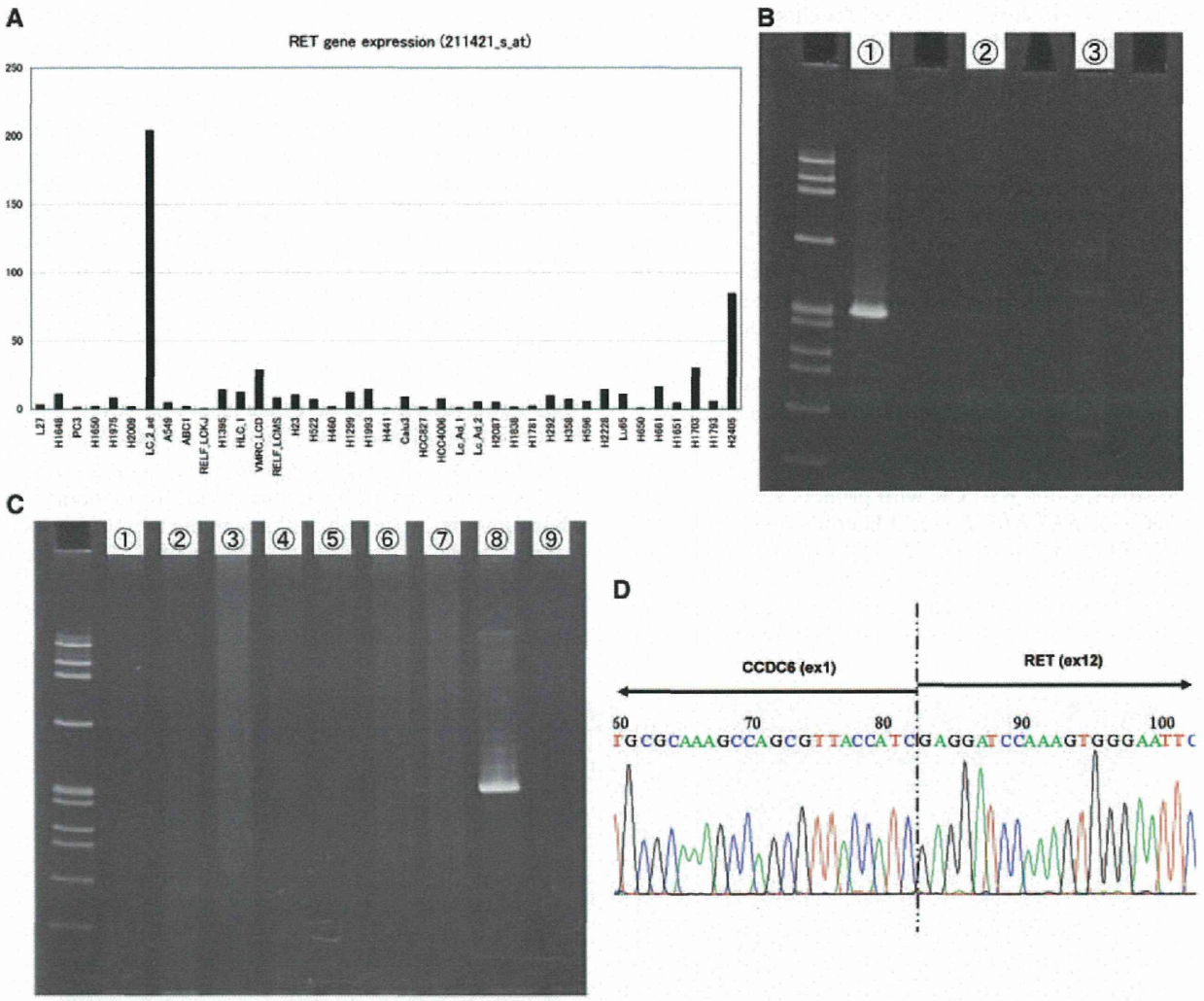

FIGURE 3. Identification of *CCDC6-RET* fusion in LC-2/ad by fusion-specific RT-PCR. *A*, Bar graphs of gene-level expressions of RET in the 39 cell lines. *B*, Results for fusion-specific RT-PCR of LC-2/ad: with the forward primer *CCDC6*-197F and reverse primer *RET*-2381R (Lane 1), with the forward primer *KIF5B*-867F and reverse primer *RET*-2381R (Lane 2), and with the forward primer KIF5B-2265F and reverse primer *RET*-2381R (Lane 3). A PCR product of an expected size (352 base pair) was amplified in Lane 1, but not in Lane 2 or Lane 3. Molecular weight marker: φX174-HAE digest. *C*, RET-CCDC6 fusion was captured only in LC-2/ad and was not captured in any of the other cell lines tested. The results for eight cell lines are shown: Lane 1, A549; Lane 2, ABC1; Lane 3, Calu-3; Lane 4, PC3; Lane 5, RERF-LC-KJ; Lane 6, HLC-1; Lane 7, L27; Lane 8, LC-2/ad; and Lane 9, VMRC-LCD). Molecular weight marker: φX174-HAE digest. *D*, Direct sequencing of the PCR product containing *RET-CCDC6* fusion. PCR, polymerase chain reaction; RT-PCR, reverse-transcriptase polymerase chain reaction.

RESULTS AND DISCUSSION

Sensitivity of Non–Small-Cell Carcinoma Cell Lines to Vandetanib and Gefitinib

We examined and compared the efficacy of vandetanib (ZD6474) and gefitinib (both provided by AstraZeneca, London, England) in 39 non–small lung carcinoma cell lines (Supplementary Figure 1, Supplemental Digital Content 2, http://links.lww.com/JTO/A338). Most cell lines showed similar sensitivities to the two kinase inhibitors; however, a notable exception was the lung adenocarcinoma, LC-2/ad, which was resistant to gefitinib, but highly sensitive to vandetanib. To illustrate this distinctive feature of LC-2/ad, the dose-response curves of LC-2/ad for gefitinib and vandetanib are shown in Figure 1, together with those of HCC827 (an *EGFR*-mutated cell line) and H1993 (an *MET*-amplified cell line).

Effects of Vandetanib on the Phosphorylation of Downstream Effectors of Growth Factor Receptors, ERK and AKT of LC-2/ad

We tested the effects of vandetanib and gefitinib treatments on ERK and AKT signaling in LC-2/ad, HCC827, and H1993. Results are shown in Figure 2. Vandetanib (1×10^{-6} M) effectively abolished baseline phosphorylation of ERK and AKT in both LC-2/ad and HCC827, but not in H1993. In

Copyright © 2012 by the International Association for the Study of Lung Cancer

contrast, gefitinib effectively abolished baseline phosphorylation of ERK and AKT only in HCC827. This suggests that, in LC-2/ad, ERK and AKT are activated through a vandetanib-sensitive pathway other than EGFR signaling.

Identification of *RET* Fusion in LC-2/ad.

Among the tyrosine kinases targeted by vandetanib, RET was an obvious candidate molecule. First, in our oligonucleotide array analysis data of 39 cell lines, LC/2-ad showed lower expressions of vascular endothelial growth factor receptor-2 and EGFR, but distinctively higher expression of RET than that of other cell lines (Fig. 3A and Supplementary Data 1, Supplemental Digital Content 3, http://links.lww.com/JTO/A339). Second, the result of an independently performed exon array analysis of LC-2/ad suggested the existence of *RET* fusion in LC-2/ad (not shown).

To directly demonstrate *RET* fusion in LC-2/ad, we performed fusion-specific RT-PCR with primers sets that detect *RET-CCDC6* or *RET-KIF5B* (see Materials and Methods).[4] *RET-CCDC6* fusion, but not *RET-KIF5B* fusion, was detected in LC-2/ad. No PCR product was amplified in any of the other cell lines examined (Fig. 3*B* and *C*). Direct sequence analysis of RT-PCR products demonstrated a fusion between *CCDC6* exon1 and *RET* exon12 (Fig. 3*D*). An independently performed 5′ rapid amplification of complementary DNA ends (5′-RACE) using a primer complementary to *RET* demonstrated the same fusion in LC-2/ad (data not shown). Although *CCDC6-RET* fusions have now been found in many lung cancers, these cases have the same breakpoints; exon 1 of *CCDC6* is fused to exon 12 of *RET* at the cDNA level. The thyroid cancer cell line TPC-1 also harbors *CCDC6-RET* fusion at the same site.[14] However, we have not checked the breakpoints of the *RET* and *CCDC6* genes in LC-2/ad at the genomic level. Thus, it would be of interest to further determine and characterize the genomic breakpoints in *CCDC6-RET* fusion–positive tumors.

Histopathologic Characteristics of an Established Xenograft Tumor of LC-2/ad

LC-2/ad was established from the pleural effusion of a 51-year-old female pulmonary adenocarcinoma patient whose smoking status was unknown; the tumor histology was reported to be a moderately differentiated adenocarcinoma with distinct glandular structures.[15] To confirm this earlier finding and to further examine the histopathologic features of this cell line, we established a xenograft tumor of LC-2/ad

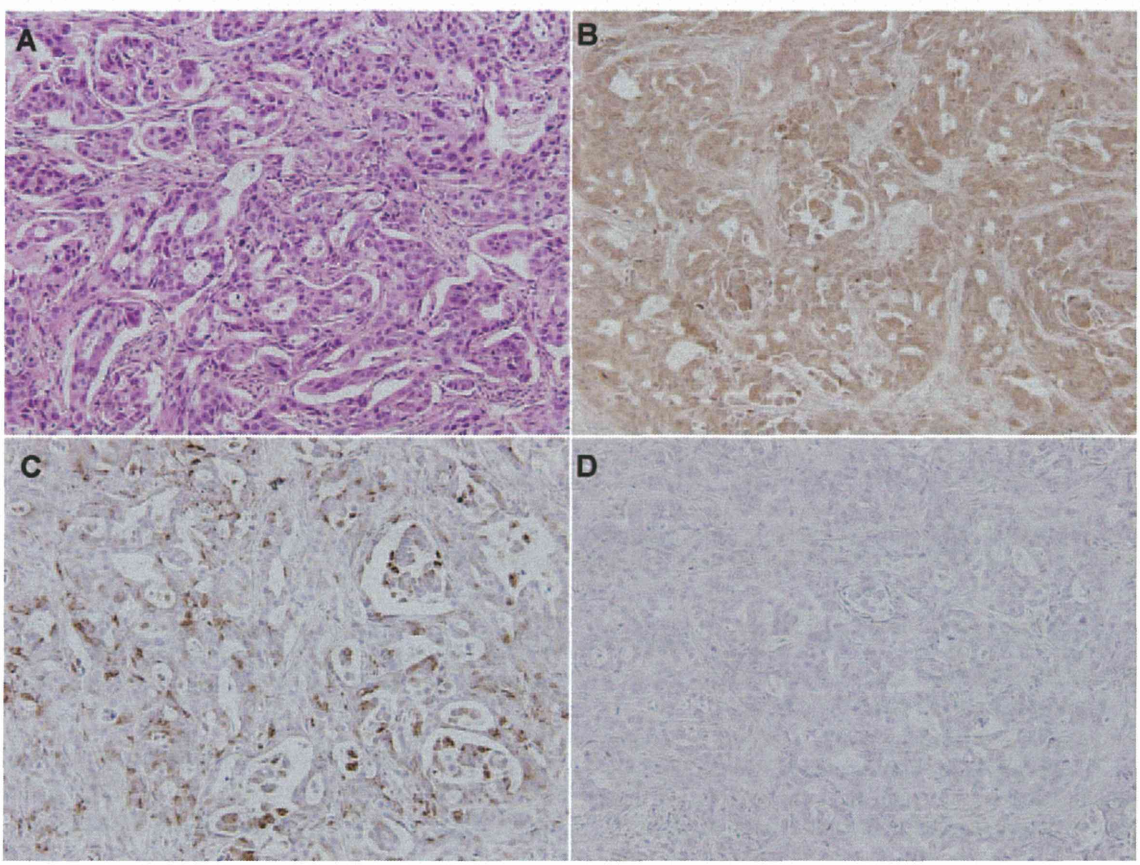

FIGURE 4. Histopathologic characteristics of an established xenograft tumor of LC-2/ad. *A*, The main histopathologic diagnosis of the tumor was acinar-predominant adenocarcinoma showing a cribriform pattern (hematoxylin and eosin staining, ×200). *B*, The tumor was positive for RET (RET immunostaining, ×200). *C*, The tumor was positive for Napsin A (Napsin A immunostaining, ×200). *D*, The tumor was negative for thyroglobulin (Thyroglobulin immunostaining, ×200).

Copyright © 2012 by the International Association for the Study of Lung Cancer